2011 50th IEEE Conference on Decision and Control and
European Control Conference (CDC-ECC)
Orlando, FL, USA, December 12-15, 2011

Robust nonlinear control design for a minimally-actuated flapping-wing MAV in the longitudinal plane

Andrea Serrani

Abstract— **We present in this paper the design of a nonlinear controller for robust control of an insect-like flapping-wing MAV model in the longitudinal plane. Only two forms of actuation are employed in the model considered herein: (i) variable wing-beat frequency and (ii) variable stroke plane angle, which result in an under-actuated model. Methodologies from averaging theory and tracking by bounded feedback are combined for the design of a controller of fixed structure that provides robust stabilization of a time-averaged vehicle model to a desired constant configuration. For the actual vehicle model, this method provides robust stabilization of a small-amplitude periodic orbit centered at the setpoint, as verified in simulation.**

I. INTRODUCTION

Small-scale, biologically-inspired MAVs have the potential to achieve a level of performance unattainable by fixed- or rotary-wing UAVs, both in terms of agility and resilience to environmental disturbance, as well as in the capability of performing advanced maneuvers like perching. Achieving these kinds of biologically-inspired behaviors on robotic MAVs comprises a formidable series of tasks, which encompasses designing and sizing the actual vehicle [1], [2], modeling the complex aerodynamics of flapping-wing flight [3], equipping the vehicle with a suitable set of actuators and sensors [4], and finally designing flight control algorithms [5]. From the point of view of control system design, one of the most outstanding issues inherent in flapping wing flight is the requirement of periodically-varying actuation, which gives rise to time-varying models that are difficult to analyze. Unconventional forms of actuation, such as moving appendages to change instantaneously the vehicle moment of inertia or weight-shifting mechanisms to alter the location of the center of gravity, may become necessary to achieve the degree of maneuverability expected from this class of vehicles [6], [7]. However, due to stringent size and weight constraints, a minimally-actuated vehicle is a preferred choice, which comes at the expenses of under-actuated dynamics resulting often in non-minimum phase behaviors. In the recent work [8], a rigorous framework was established in which averaging theory and stabilization by bounded feedback is combined for the definition of a robust control strategy with low computational cost to control a 1-DOF MAV model in hover. A first attempt to extend this methodology to a minimally-actuated 3-DOF vehicle model derived by restricting the 6-DOF model of [9] to the longitudinal plane, was presented in [10]. The resulting controller was observed in simulation to provide only local convergence to a desired configuration, and suffered from poor robustness and small stability margins. In particular, the controller failed to provide adequate stabilization of the weakly unstable internal dynamics. In this paper, we present a complete redesign of a robust controller for the same 3-DOF model of the generic insect-like MAV of [9]. The controller is based on a novel transformation involving the control inputs and involves the use of a saturated dynamic extension to manage the non-minimum phase behavior of the model. Simulation results show a drastic improvement over previous results in tracking performance and robustness.

The paper is organized as follows: In Section II, the vehicle model is introduced, and the averaged model developed. The controller design and a sketch of the stability analysis are presented in Section III. Simulation results are discussed in Section IV, whereas conclusions are offered in Section V.

II. VEHICLE MODEL AND ANALYSIS

The equations of motion of the 6-DOF MAV dynamics of [9], when restricted to the longitudinal plane (see Figure 1) are given by:

$$\begin{aligned}
\ddot{x} &= \frac{k}{m}\dot{\mu}^2 \left[C_L(\alpha)\sin(\lambda-\theta)\right. \\
&\qquad \left. -\mathrm{sign}(\dot{\mu})C_D(\alpha)\cos(\mu)\cos(\lambda-\theta)\right] \\
\ddot{z} &= g - \frac{k}{m}\dot{\mu}^2 \left[C_L(\alpha)\cos(\lambda-\theta)\right. \\
&\qquad \left. +\mathrm{sign}(\dot{\mu})C_D(\alpha)\cos(\mu)\sin(\lambda-\theta)\right] \\
\ddot{\theta} &= \frac{k}{I_{yy}} \left[C_D(\alpha)\cos(\mu)\mathrm{sign}(\dot{\mu})\left(x_r\cos(\epsilon)+r_z\cos(\lambda)\right.\right. \\
&\qquad \left. +r_x\sin(\lambda)\right) C_L(\alpha)\left(r_x\cos(\lambda)-x_r\cos(\mu)\sin(\epsilon)\right. \\
&\qquad \left.\left. -r_z\sin(\lambda)+y_r\sin(\mu)\right)\right] \qquad (1)
\end{aligned}$$

where (x, z, θ) are respectively the longitudinal and vertical position of the center of mass and the pitch angle of the vehicle with respect to an inertial coordinate system. For convenience, we denote by $\boldsymbol{x} = [x, \dot{x}, z, \dot{z}, \theta, \dot{\theta}]$ the state vector of (1). It is assumed that the angle-of-attack of the wings, α, is constant along the span of both the upstroke and downstroke. The vectors $[x_r, y_r]$ and $[r_x, r_z]$ are constant vehicle parameters, whereas μ is the time-varying wing beat and $\epsilon = -\mathrm{sign}\,(\dot{\mu})\,(\pi/2-\alpha)$. Finally, g, m and I_{yy} denote respectively acceleration of gravity, mass and moment of inertia about the body-y axis. Here, as opposed to [9], we

This work was supported by AFRL through a subcontract from the Collaborative Center of Control Science at the University of Michigan and through the AFRL Summer Faculty Fellowship Program.

Andrea Serrani is with the Department of Electrical & Computer Engineering, 2015 Neil Ave., The Ohio State University, Columbus, OH, 43210.

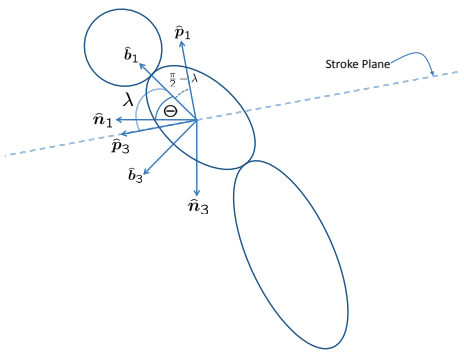

Fig. 1. Schematics of the multi-body MAV of [9] in the (x, z)-plane.

assume that the tail is not actuated and is not a degree of freedom. Therefore, this longitudinal vehicle model is equipped with a minimal set of two control inputs; the first one acts through the wing beat

$$\mu(t) = \sin(\omega_0 t + \Delta) \tag{2}$$

where $\omega_0 > 0$ is a given constant carrier frequency and Δ is a phase shift whose derivative can be manipulated by the control system. The stroke plane angle, λ, acts as the second control effector. It is required that $|\mathrm{d}\Delta/\mathrm{d}t| < \omega_0$ to maintain periodicity of the wing beat, whereas λ is bound to range over the interval $[0, \pi/2]$. The output to be controlled is selected as the position of the center of mass, $\boldsymbol{y} = [x, z]$. Letting $\delta := \dot{\Delta}/\omega_0$, $|\delta| < 1$, and keeping in mind (2) one obtains the following representation of system (1)

$$\begin{aligned} \dot{\boldsymbol{x}} &= f(t, \boldsymbol{x}, \boldsymbol{v}) \\ \boldsymbol{y} &= h(\boldsymbol{x}) \end{aligned} \tag{3}$$

where $\boldsymbol{v} = [\delta, \lambda]$. The control input is to be provided by a smooth time-invariant state-feedback controller of the form

$$\begin{aligned} \dot{\boldsymbol{\xi}} &= F(\boldsymbol{\xi}, \boldsymbol{x}, \boldsymbol{y}_d) \\ \boldsymbol{v} &= H(\boldsymbol{\xi}, \boldsymbol{x}, \boldsymbol{y}_d) \end{aligned} \tag{4}$$

where $\boldsymbol{\xi} \in \mathbb{R}^\nu$, $H(\cdot)$ is a *bounded function* of its arguments and $\boldsymbol{y}_d = [x_d, z_d]$ is a desired setpoint for the output. Note that the controller does depend explicitly on t.

A. Averaged model

Following the procedure outlined in [8] for a 1-DOF MAV model, the dynamics (3)-(4) are time-rescaled and averaged to obtain a suitable averaged model. Since by assumption $|\delta| < 1$, the time re-scaling $t' = t + \int_0^t \delta(\tau)\mathrm{d}\tau$ is well defined, and it is easy to verify that $\frac{\mathrm{d}}{\mathrm{d}t} = (1+\delta)\frac{\mathrm{d}}{\mathrm{d}t'}$, $\frac{\mathrm{d}}{\mathrm{d}t'} = \frac{1}{1+\delta}\frac{\mathrm{d}}{\mathrm{d}t}$. Since typically $\omega_0 >> 1$ and $m/k >> 1$, by setting $\omega_0 = 1/\varepsilon$ and regarding $\sqrt{m/k} = \mathcal{O}(\varepsilon)$ (which implies that ω_0^2 scales with the ratio m/k), one obtains

$$\frac{k}{m}\dot{\mu}^2(t) = \frac{k}{m}\,\varepsilon^2\big(1 + \delta(\boldsymbol{x})\big)^2 \cos^2\left(\frac{t'}{\varepsilon}\right)$$

As a result, system (3)-(4) is in the appropriate form for averaging with respect to the time variable t'. Applying the averaging operator $\mathrm{avg}\,(u) := \frac{\omega_0}{2\pi}\int_0^{2\pi/\omega_0} u\,(t')\,\mathrm{d}t'$ to the right-hand side of (3)-(4) and reverting back to the natural time scale, one obtains the *averaged plant model*

$$\begin{aligned} \ddot{x} &= \frac{k_L\omega_0^2}{2m}(1+\delta)^2\sin(\lambda - \theta) \\ \ddot{z} &= g - \frac{k_L\omega_0^2}{2m}(1+\delta)^2\cos(\lambda - \theta) \\ \ddot{\theta} &= \frac{\rho_r k_L\omega_0^2}{2I_{yy}}(1+\delta)^2\cos(\lambda + \lambda_r) \end{aligned} \tag{5}$$

where $k_L := kC_L(\alpha)$, $\rho_r := \sqrt{r_x^2 + r_z^2}$ and $\lambda_r := \tan^{-1}(r_z/r_x)$. It is assumed that $\rho_r > 0$ and $\lambda_r \in (0, \pi/2)$. Obviously, the controller model is invariant under averaging. Finally, letting

$$\beta_1 := \frac{k_L\omega_0^2}{2m},\ \beta_2 := \frac{\rho_r k_L\omega_0^2}{2I_{yy}},\ \omega_* := \sqrt{\frac{2mg}{k_L}},\ \lambda_* := \frac{\pi}{2} - \lambda_r$$

one obtains

$$\begin{aligned} \ddot{x} &= \beta_1(1+\delta)^2\sin(\lambda - \theta) \\ \ddot{z} &= \beta_1\left[\frac{\omega_*^2}{\omega_0^2} - (\delta+1)^2\cos(\lambda - \theta)\right] \\ \ddot{\theta} &= -\beta_2(1+\delta)^2\sin(\lambda - \lambda_*) \end{aligned} \tag{6}$$

It goes without saying that the parameters $\beta_1 > 0$, $\beta_2 > 0$ and $\omega_* > 0$ are affected by uncertainty, and are hereby assumed to range over appropriate known compact intervals. In particular, we set $0 < \underline{\beta}_1 \le \beta_1 \le \bar{\beta}_1$, $0 < \underline{\beta}_2 \le \beta_2 \le \bar{\beta}_2$. Due to the limits imposed on λ and λ_r, the averaged system (6) has an unstable equilibrium at $(x, z, \theta) = (x_d, z_d, \lambda_*)$ provided that $\delta = \omega_*/\omega_0 - 1$ and $\lambda = \lambda_*$. This equilibrium corresponds to a periodic orbit for the original system [11]. By the average theorem, exponential stabilization of the given equilibrium for (6) corresponds to stabilization of the ensuing periodic orbit for (3).

Note that ω_* is the value of the angular frequency of the wing beat that maintains the vehicle in hovering condition, which must be reconstructed by the controller to provide the equilibrium condition. Finally, it is readily seen that system (6) is weakly non-minimum phase with respect to $\boldsymbol{y}$, since the corresponding zero dynamics

$$\ddot{\theta} = -\beta_2\frac{\omega_*^2}{\omega_0^2}\sin(\theta - \lambda_*)$$

have a center at $(\theta, \dot{\theta}) = (\lambda_*, 0)$.

III. CONTROLLER DESIGN

To begin, we extend the input λ with the chain of integrators

$$\begin{aligned} \dot{\lambda}_1 &= \lambda_2 \\ \dot{\lambda}_2 &= u_2\,, \quad \lambda = \ell^\lambda\,\mathrm{sat}\left(\frac{\lambda_1}{\ell^\lambda}\right) + \lambda_* \end{aligned} \tag{7}$$

with state $\boldsymbol{\lambda} = [\lambda_1, \lambda_2]$, where $\ell^\lambda := \min\{\pi/2 - \lambda_*, \lambda_*\}$, and define the new control input as $\boldsymbol{u} = [u_1, u_2] := [\delta, u_2]$. As in [12], a *unit saturation function* $\mathrm{sat} : \mathbb{R} \to \mathbb{R}$ is a twice-differentiable function satisfying the following properties:

Property 3.1 (Properties of the saturation function):

$|\,\mathrm{sat}'(s)| := |\mathrm{d}\,\mathrm{sat}(s)/\mathrm{d}s| \le 2$ *for all* s

$|\,\mathrm{sat}''(s)| := |\mathrm{d}^2\,\mathrm{sat}(s)/\mathrm{d}s^2| \le K$ *for all* s, $K > 0$

$s\,\mathrm{sat}(s) > 0$ *for all* $s \neq 0$, $\mathrm{sat}(0) = 0$

$\mathrm{sat}(s) = \mathrm{sign}(s)$ *for* $|s| \ge 1$

$|s| < |\,\mathrm{sat}(s)| < 1$ *for* $|s| < 1$

Note that the above choice for the saturation level ℓ^λ enforces the bound $\lambda \in [0, \pi/2]$. The overall multi-loop controller architecture is comprised of three control loops, the innermost being the third. In the first-level loop, the wing-beat and the pitch dynamics act as servo-controllers for the longitudinal and vertical dynamics generating the output to be regulated, whereas the output of the dynamic extension plays the role of a disturbance. On the other hand, the second-level loop regulates the pitch dynamics servo-controller via the output of the dynamic extension, which is then controlled by the third-level loop compensator. The dynamic extension becomes necessary to circumvent the appearance of λ in the longitudinal/vertical dynamics and to mitigate the non-minumum phase effect.

A. First-level loop controller

Applying the *change of coordinates* $\eta := \lambda - \theta$ (which is well-defined, due to the dynamic extension) and the "polar-to-cartesian" transformation $(u_1, \eta) \mapsto (v_x, v_z)$ defined as

$$v_x := (1+u_1)^2 \sin(\eta)\,, \quad v_z := 1 - (1+u_1)^2 \cos(\eta) \quad (8)$$

the longitudinal and vertical dynamics have the particularly simple expression

$$\begin{aligned} \ddot{x} &= \beta_1 v_x \\ \ddot{z} &= \beta_1 (v_z + r_\omega) \end{aligned} \quad (9)$$

where $r_\omega := \omega_*/\omega_0 - 1$ is a constant uncertain term to be compensated. In (9), v_x and v_z play the role of (bounded) virtual inputs, as neither of them can be directly assigned due to their implicit dependence on θ through η. Note that the transformation (8) is defined globally on $(u_1, \eta) \in (-1, 1) \times (-\pi/2, \pi/2)$ and is invertible if v_z satisfies $|v_z| < 1$, since it entails $\eta = \arctan(v_x/(1 - v_z))$. Next, bounded controls

$$\left|v_x^{cmd}\right| \le \bar{v}_x\,, \quad \left|v_z^{cmd}\right| \le \bar{v}_z \quad (10)$$

are determined to robustly stabilize the setpoint $\boldsymbol{y}_d$ when $[v_x, v_z] = [v_x^{cmd}, v_z^{cmd}]$. The bounds $\bar{v}_x > 0$ and $\bar{v}_z > 0$ must be selected such that[1] $|v_x| \le \bar{v}_x$ and $|v_z| \le \bar{v}_z \implies |u_1| \le \bar{u}_1$ and $|\eta| \le \bar{\eta}$ for some $\bar{u}_1 \in (0, 1)$ and $\bar{\eta} \in (0, \pi/2)$. Using the identity $(1+u_1)^2 = v_x^2 + (1 - v_z)^2$, one can prove that the selection

$$\bar{v}_x = \frac{1}{\sqrt{2}}(1+\bar{u}_1)^2\,, \quad \bar{v}_z = \frac{1}{\sqrt{2}}(1+\bar{u}_1)^2 - 1$$

parameterized by the bound $\bar{u}_1$ is a valid choice, as long as one takes $\bar{u}_1 \in (2^{1/4}, 1) \approx (0.19, 1)$. Note that the second bound in (10) inevitably restricts to a fraction of $\bar{v}_z$ the maximum parametric uncertainty r_ω that can be tolerated.

The design of the virtual controls v_x^{cmd}, v_z^{cmd} follows standard methodologies based on nested-saturation design. In particular, we adopt the one proposed in [12] for uncertain chains of integrators. For the x-dynamics, letting $x_1 := x - x_d$, $x_2 := \dot{x} + \ell_1^x\,\mathrm{sat}\left(\frac{\kappa_1^x}{\ell_1^x} x_1\right)$ and selecting

$$v_x^{cmd} := -\ell_2^x\,\mathrm{sat}\left(\frac{\kappa_2^x}{\ell_2^x} x_2\right) \quad (11)$$

where $\ell_i^x > 0$, $\kappa_i^x > 0$, $i = 1, 2$, are parameters, one obtains

$$\begin{aligned} \dot{x}_1 &= -\ell_1^x\,\mathrm{sat}\left(\frac{\kappa_1^x}{\ell_1^x} x_1\right) + x_2 \\ \dot{x}_2 &= \beta_1 \left[d_x - \ell_2^x\,\mathrm{sat}\left(\frac{\kappa_2^x}{\ell_2^x} x_2\right)\right] + \kappa_1^x\,\mathrm{sat}'\left(\frac{\kappa_1^x}{\ell_1^x} x_1\right)\dot{x}_1 \end{aligned} \quad (12)$$

where, obviously, $d_x := v_x - v_x^{cmd}$.

Proposition 3.2: Let the gains κ_1^x and ℓ_1^x be parameterized as follows

$$\kappa_1^x = \varepsilon_1^x \kappa_2^x, \qquad \ell_1^x = (1 - a_1^x)\frac{\ell_2^x}{\kappa_2^x} + a_1^x\,\frac{\underline{\beta}_1 \ell_2^x}{4\,\varepsilon_1^x \kappa_2^x}$$

where $\varepsilon_1^x \in \left(0, \underline{\beta}_1/4\right)$ and $a_1^x \in (0, 1)$. Then, for any $\kappa_2^x > 0$ and any $\ell_2^x \in (0, \bar{v}_x]$ the system (12) is ISS from the set $\mathcal{X}_x = \mathbb{R}^2$ with restriction $\Delta_x = \ell_2^x/2$ on the disturbance d_x. Furthermore, the state satisfies the asymptotic bounds

$$\|x_1\|_a \le \frac{2}{\kappa_1^x \kappa_2^x}\|d_x\|_a\,, \quad \|x_2\|_a \le \frac{2}{\kappa_2^x}\|d_x\|_a \quad (13)$$

Proof: The proof follows directly from the arguments in [12] (see also [13]) and are thus omitted for brevity. ■

For the z-dynamics, we first augment the second equation in (9) with the integral error $\dot{z}_1 = z - z_d$ and then apply the change of coordinates

$$z_2 := z - z_d + \ell_1^z\,\mathrm{sat}\left(\frac{\kappa_1^z}{\ell_1^z} z_1\right), \quad z_3 := \dot{z} + \ell_2^z\,\mathrm{sat}\left(\frac{\kappa_2^z}{\ell_2^z} z_2\right)$$

and select the virtual control

$$v_z^{cmd} := -\ell_3^z\,\mathrm{sat}\left(\frac{\kappa_3^z}{\ell_3^z} z_3\right)$$

where $\ell_i^z > 0$, $\kappa_i^z > 0$, $i = 1, \ldots, 3$, are design parameters. The resulting expression of the augmented system reads as

$$\begin{aligned} \dot{z}_1 &= -\ell_1^z\,\mathrm{sat}\left(\frac{\kappa_1^z}{\ell_1^z} z_1\right) + z_2 \\ \dot{z}_2 &= -\ell_2^z\,\mathrm{sat}\left(\frac{\kappa_2^z}{\ell_2^z} z_2\right) + z_3 + \kappa_1^z\,\mathrm{sat}'\left(\frac{\kappa_1^z}{\ell_1^z} z_1\right)\dot{z}_1 \\ \dot{z}_3 &= \beta_1 \left[d_z - \ell_3^z\,\mathrm{sat}\left(\frac{\kappa_3^z}{\ell_3^z} z_3\right) + r_\omega\right] + \kappa_2^z\,\mathrm{sat}'\left(\frac{\kappa_2^z}{\ell_2^z} z_2\right)\dot{z}_2 \end{aligned} \quad (14)$$

where $d_z := v_z - v_z^{cmd}$. The analogous to Proposition 3.2 for system (14) is stated as follows:

Proposition 3.3: Let the gains κ_i^z, ℓ_i^z, $i = 1, 2$, be parameterized as follows

$$\kappa_1^z = \varepsilon_1^z \kappa_2^z, \qquad \ell_1^z = (1 - a_1^z)\frac{\ell_2^z}{\kappa_2^z} + a_1^z\,\frac{\ell_2^z}{4\,\varepsilon_1^z \kappa_2^z}$$

$$\kappa_2^z = \varepsilon_2^z \kappa_3^z, \qquad \ell_2^z = (1 - a_2^z)\frac{2\ell_3^z}{\kappa_3^z} + a_2^z\,\frac{\underline{\beta}_1 \ell_3^z}{6\,\varepsilon_2^z \kappa_3^z}$$

[1] It should be noted that these bound are only enforced for $[v_x^{cmd}, v_z^{cmd}]$. For the actual variables $[v_x(t), v_z(t)]$, it suffices that the bounds hold ultimately, that is, for all $t \ge T$, for some $T > 0$.

where $\varepsilon_1^z \in \left(0, \frac{1}{4}\right)$, $\varepsilon_2^z \in \left(0, \frac{\beta}{12}\right)$, $a_1^z \in (0,1)$, $a_2^z \in (0,1)$. Then, for any $\kappa_3^z > 0$ and any $\ell_3^z \in (0, \bar{v}_z]$ the system (12) is ISS from the set $\mathcal{X}_z = \mathbb{R}^3$ with restrictions $\Delta_z = \ell_3^z/3$, $\Delta_\omega = \ell_3^z/3$ on the disturbance inputs d_z and r_ω, respectively. Furthermore, for any *constant* r_ω satisfying $|r_\omega| < \Delta_\omega$, system (14) has a globally asymptotically and locally exponentially stable equilibrium at

$$z_1^* = \frac{r_\omega}{\kappa_1^z \kappa_2^z \kappa_3^z}, \quad z_2^* = \frac{r_\omega}{\kappa_2^z \kappa_3^z}, \quad z_3^* = \frac{r_\omega}{\kappa_3^z}$$

whenever $d_z = 0$. For arbitrary signals d_z satisfying $\|d_z\|_a < \Delta_z$, the state in the *error coordinates* $\tilde{z}_1 := z_1 - z_1^*$, $\tilde{z}_2 := z_2 - z_2^*$, $\tilde{z}_3 := z_3 - z_3^*$ satisfies the asymptotic bounds

$$\|\tilde{z}_1\|_a \le \frac{4}{\kappa_1^z \kappa_2^z \kappa_3^z}\|d_z\|_a, \quad \|\tilde{z}_2\|_a \le \frac{4}{\kappa_2^z \kappa_3^z}\|d_z\|_a$$
$$\|\tilde{z}_3\|_a \le \frac{2}{\kappa_3^z}\|d_z\|_a \tag{15}$$

Proof: The proof follows from arguments similar to those used in [12] and [8], and are thus omitted here. ∎

B. Second-level inner-loop controller

The second level of our multi-loop design is comprised of a servo-controller to achieve asymptotic regulation of the "disturbance" d_x and d_z, appearing respectively in (12) and (14). By way of the transformation (8), since u_1 can be manipulated directly, this involves letting η to track asymptotically its commanded trajectory $\eta_{cmd} := \arctan\left(\frac{v_x^{cmd}}{1 - v_z^{cmd}}\right)$. By definition of η, it follows that this objective must be achieved by controlling the pitch dynamics. Define the change of coordinates $(\eta, \dot{\theta}) \mapsto (\eta_1, \eta_2)$ as

$$\eta_1 := \eta_{cmd} - \eta = \eta_{cmd} + \theta - \lambda$$
$$\eta_2 := \dot{\theta} - \dot{\lambda} + \ell_1^\eta \operatorname{sat}\left(\frac{\kappa_1^\eta}{\ell_1^\eta}\eta_1\right)$$

where $\ell_1^\eta > 0$ and κ_1^η are design parameters. For the resulting dynamics

$$\dot{\eta}_1 = -\ell_1^\eta \operatorname{sat}\left(\frac{\kappa_1^\eta}{\ell_1^\eta}\eta_1\right) + \eta_2 + \dot{\eta}_{cmd}$$
$$\dot{\eta}_2 = -\beta_2(1+u_1)^2 \sin\left(\ell^\lambda \operatorname{sat}\left(\frac{\lambda_1}{\ell^\lambda}\right)\right) - \frac{1}{\ell^\lambda}\operatorname{sat}''\left(\frac{\lambda_1}{\ell^\lambda}\right)\lambda_2$$
$$- \operatorname{sat}'\left(\frac{\lambda_1}{\ell^\lambda}\right)u_2 + \kappa_1^\eta \operatorname{sat}'\left(\frac{\kappa_1^\eta}{\ell_1^\eta}\eta_1\right)\dot{\eta}_1$$

the state λ_1 plays the role of a virtual control input, whose "commanded value" is $\lambda_1^{cmd} := \ell_2^\eta \operatorname{sat}\left(\frac{\kappa_2^\eta}{\ell_2^\eta}\eta_2\right)$, $\ell_2^\eta, \kappa_2^\eta > 0$. This yields the system

$$\dot{\eta}_1 = -\ell_1^\eta \operatorname{sat}\left(\frac{\kappa_1^\eta}{\ell_1^\eta}\eta_1\right) + \eta_2 + \dot{\eta}_{cmd}$$
$$\dot{\eta}_2 = -\beta_2(1+u_1)^2 \sin\left(\ell^\lambda \operatorname{sat}\left(\frac{\ell_2^\eta \operatorname{sat}\left(\frac{\kappa_2^\eta}{\ell_2^\eta}\eta_2\right) + \tilde{\lambda}_1}{\ell^\lambda}\right)\right)$$
$$+ d_\lambda + \kappa_1^\eta \operatorname{sat}'\left(\frac{\kappa_1^\eta}{\ell_1^\eta}\eta_1\right)\dot{\eta}_1 \tag{16}$$

where $\tilde{\lambda}_1 := \lambda_1 - \lambda_1^{cmd}$ and $d_\lambda := \frac{1}{\ell^\lambda}\operatorname{sat}''\left(\frac{\lambda_1}{\ell^\lambda}\right)\lambda_2 - \operatorname{sat}'\left(\frac{\lambda_1}{\ell^\lambda}\right)u_2$. For the sake of simplicity we take $\ell_2^\eta = \ell^\lambda$. To analyze the asymptotic properties of the above system, we use the following "basic saturation lemma":

Lemma 3.4: The scalar system

$$\dot{x} = -a\,\ell_1 \operatorname{sat}\left(\left(\frac{\ell_2}{\ell_1}\operatorname{sat}\left(\frac{k_2}{\ell_2}x\right) + \frac{d_1}{\ell_1}\right)\right) + d_2$$

where $a > 0$, $\ell_i > 0$, $i = 1, 2$, and $k_2 > 0$ is ISS from the set $\mathcal{X} = \mathbb{R}$ with restrictions $\Delta_1 = \ell_2/2$, $\Delta_2 = \min\{a\ell_1, a\ell_2/2\}$ on the inputs d_1, d_2, respectively. Furthermore, the state satisfies the asymptotic bound $\|x\|_a \le \frac{2}{k_2}\max\left\{\|d_1\|_a, \frac{1}{a}\|d_2\|_a\right\}$.

Proof: The proof follows from the results in [14]. ∎

The asymptotic behavior of system (16) is described in the following proposition, whose proof can be obtained by combining the results of [12] and Lemma 3.4:

Proposition 3.5: Let κ_i^η, ℓ_i^η, $i = 1, 2$, be parameterized as

$$\kappa_1^\eta = \varepsilon_1^\eta \kappa_2^\eta$$
$$\ell_2^\eta = \ell_\lambda, \quad \ell_1^\eta = 2(1 - a_1^\eta)\frac{\ell_\lambda}{\kappa_2^\eta} + a_1^\eta \frac{\underline{\beta}_2(1-\bar{u}_1)^2\ell_\lambda}{8\,\varepsilon_1^\eta \kappa_2^\eta}$$

where $\varepsilon_1^\eta \in \left(0, \frac{\underline{\beta}_2(1-\bar{u}_1)^2}{16}\right)$, $a_1^\eta \in (0,1)$. Then, for any $\kappa_2^\eta > 0$, system (16) is ISS from the set $\mathcal{X}_\eta = \mathbb{R}^2$, with restriction $\Delta_{\dot{\eta}_{cmd}} = \ell_1^\eta/2$ on $\dot{\eta}_{cmd}$, restriction $\Delta_{\tilde{\lambda}_1} = \ell_\lambda/2$ on $\tilde{\lambda}_1$, and restriction $\Delta_\lambda = \underline{\beta}_2(1-\bar{u}_1)^2\ell_\lambda/2$ on d_λ, respectively. Furthermore, the state satisfies the asymptotic bounds

$$\|\eta_1\|_a \le \frac{2}{\kappa_1^\eta}\max\left\{\frac{2}{\kappa_2^\eta}\|\tilde{\lambda}_1\|_a, \|\dot{\eta}_{cmd}\|_a, \frac{8\kappa_1^\eta}{\kappa_2^\eta \underline{\beta}_2(1-\bar{u}_1)^2}\|d_\lambda\|_a\right\}$$
$$\|\eta_2\|_a \le \frac{2}{\kappa_2^\eta}\max\left\{\|\tilde{\lambda}_1\|_a, \frac{4\kappa_1^\eta}{\underline{\beta}_2(1-\bar{u}_1)^2}\|\dot{\eta}_{cmd}\|_a \frac{4\kappa_1^\eta}{\underline{\beta}_2(1-\bar{u}_1)^2}\|d_\lambda\|_a\right\} \tag{17}$$

C. Third-level loop

The third-level loop involves the states of the dynamic extension. Letting, in a classic backstepping fashion, $\tilde{\lambda}_2 := \lambda_2 + \kappa_1^\lambda \tilde{\lambda}_1$, $\kappa_1^\lambda > 0$, and selecting the high-gain feedback $u_2 = -(\kappa_1^\lambda + \kappa_2^\lambda)\tilde{\lambda}_2 + (\kappa_1^\lambda)^2\tilde{\lambda}_1$, $\kappa_2^\lambda > 0$, one obtains

$$\dot{\tilde{\lambda}}_1 = -\kappa_1^\lambda \tilde{\lambda}_1 + \tilde{\lambda}_2 - \dot{\lambda}_1^{cmd}$$
$$\dot{\tilde{\lambda}}_2 = -\kappa_2^\lambda \tilde{\lambda}_2 - \kappa_1^\lambda \dot{\lambda}_1^{cmd} \tag{18}$$

It should be obvious that for any $\kappa_2^\lambda > 0$ this system is ISS from $\mathcal{X}_\lambda = \mathbb{R}^2$, with no restriction on the input $\dot{\lambda}_1^{cmd}$. It is also easy to verify that the following bounds hold:

$$\|\tilde{\lambda}_1\|_a \le 2\max\left\{\frac{1}{\kappa_2^\lambda}, \frac{1}{\kappa_1^\lambda \kappa_2^\lambda}\right\}\|\dot{\lambda}_1^{cmd}\|_a, \ \|\tilde{\lambda}_2\|_a \le \frac{\kappa_1^\lambda}{\kappa_2^\lambda}\|\dot{\lambda}_1^{cmd}\|_a.$$

D. Analysis of the interconnection

Since each individual subsystem in the overall interconnection has been shown to be ISS with or without restrictions, the task is to show that for each loop there exists a choice of the available degrees of freedom (that is, those gains that can be freely assigned) such that:

1) The restrictions for the corresponding disturbance inputs are attained in finite time;
2) A small-gain involving the asymptotic norms of the coupling signals can be enforced.

If this is the case, then global asymptotic stability follows from Teel's "nonlinear small-gain theorems" for systems with saturated interconnections [15]. We will limit ourself here to provide just a sketch of the process involved. The outer interconnection has the structure of a (saturated) feedback loop between a system in strict feedback form and one in feedforward form. This type of structure has been thoroughly investigated in [13, Chapter 4], and the analysis need not be repeated here. To begin, we obtain a suitable bound for $\dot{\eta}_{cmd}$. Since $\dot{\eta}_{cmd} = \frac{1-v_z^{cmd}}{(1+u_1)^4}\dot{v}_x^{cmd} + \frac{v_x^{cmd}}{(1+u_1)^4}\dot{v}_x^{cmd}$, one obtains

$$\begin{aligned}|\dot{\eta}_{cmd}| &\leq \frac{1+\bar{v}_z}{(1-\underline{u}_1)^4}|\dot{v}_x^{cmd}| + \frac{\bar{v}_x}{(1-\underline{u}_1)^4}|\dot{v}_x^{cmd}| \\ &=: B_x|\dot{v}_x^{cmd}| + B_z|\dot{v}_x^{cmd}|\end{aligned}$$

Keeping in mind (11) and the properties of the saturation function, it can be shown that $|\dot{v}_x^{cmd}| \leq \kappa_2^x\left[\bar{\beta}_1\ell_2^x + \kappa_1^x\ell_1^x + \varepsilon_1^x\ell_2^x\right] + \kappa_2^x\bar{\beta}_1|d_x|$ Since $|d_x| \leq 2(1+\bar{u}_1)^2$, the above inequality yields $|\dot{v}_x^{cmd}| \leq \kappa_2^x N_x$, where $N_x := \bar{\beta}_1\ell_2^x + \kappa_1^x\ell_1^x + \varepsilon_1^x\ell_2^x + 2\bar{\beta}_1(1+\bar{u}_1)^2$. Similarly, it can be shown that a bound of the form $|\dot{v}_z^{cmd}| \leq \kappa_3^z N_z$ holds for $N_z := \bar{\beta}_1\ell_3^z + \bar{\beta}_1 r_\omega + 2\bar{\beta}_1(1+\bar{u}_1)^2 + \varepsilon_1^z\varepsilon_2^z\ell_3^z + \kappa_2^z\ell_2^z + \kappa_1^z\ell_2^z + \kappa_1^z\kappa_2^z\ell_1^z$. Consequently, since

$$|\dot{\eta}_{cmd}| \leq \kappa_2^x B_x N_x + \kappa_3^z B_z N_z \tag{19}$$

the restriction $\|\dot{\eta}_{cmd}\|_a < \Delta_{\dot{\eta}^{cmd}} = \ell_1^\eta/2$ can trivially be enforced for any given $\ell_1^\eta/2$ by selecting κ_2^x and κ_3^z sufficiently small (recall from Proposition 3.2 and Proposition 3.3 that these gains can be chosen arbitrarily). Moreover, from (13) and (15) it follows that

$$\|\dot{v}_x^{cmd}\|_a \leq \kappa_2^x\left(3\bar{\beta}_1 + 4\varepsilon_1^x\right)\|d_x\|_a \tag{20}$$

$$\|\dot{v}_z^{cmd}\|_a \leq \kappa_3^z\left(2\bar{\beta}_1 + 2\varepsilon_2^z + 2\varepsilon_1^z\varepsilon_2^z\right)\|d_z\|_a \tag{21}$$

Since it is easy to see that $|d_x| \leq (1+\bar{u}_1)^2|\eta_1|$ and $|d_z| \leq (1+\bar{u}_1)^2|\eta_1|$ as well, combining (19) and (20), one obtains an asymptotic bound of the form $\|\dot{\eta}_{cmd}\|_a \leq (1+\bar{u}_1)^2\left(\kappa_2^x M_x + \kappa_3^z M_z\right)\|\eta_1\|_a$. Ignoring in this analysis the interconnection with the lower subsystem, the first inequality in (17) yields $\|\eta_1\|_a \leq (2/\kappa_1^\eta)\|\dot{\eta}_{cmd}\|_a$. Consequently, we obtain the following:

1) Since $\|d_x\|_a \leq \frac{2}{\kappa_1^\eta}(1+\bar{u})^2\left(\kappa_2^x B_x N_x + \kappa_3^z B_z N_z\right)$ and similarly for $\|d_z\|_a$, the restrictions $\|d_x\|_a < \Delta_x$ and $\|d_z\|_a < \Delta_z$ are enforced by choosing κ_2^x and κ_3^z sufficiently small.
2) The condition $\frac{2}{\kappa_1^\eta}(1+\bar{u})^2\left(\kappa_2^x M_x + \kappa_3^z M_z\right) < 1$ is attained by choosing κ_2^x and κ_3^z sufficiently small.

Parameter	Value	Parameter	Value
$\bar{u}_1$	0.5	$\bar{\eta}$	1.32
$\bar{v}_x$	1.59	$\bar{v}_z$	0.59
κ_1^x	0.153	ℓ_1^x	17.5
κ_2^x	0.1	ℓ_2^x	1.59
κ_1^z	0.136	ℓ_1^z	1.73
κ_2^z	0.681	ℓ_2^z	0.96
κ_3^z	1.5	ℓ_3^z	0.59
κ_1^η	1.08	ℓ_1^η	0.3
κ_2^η	10	$\ell_2^\eta = \ell_\lambda$	0.79
κ_1^λ	20	κ_2^λ	20

TABLE I
CONTROLLER GAINS AND BOUNDS.

IV. SIMULATION RESULTS

In this section we present simulation results concerning the performance of the closed-loop system. Simulation have been carried on the *actual* vehicle model (1). The model parameters are given in [10]. A significant mismatch exists between the value of the wing-beat frequency at hover, ω_*, and the carrier frequency of the wing beat, ω_0, which underestimates the correct value by about 16%. For all other parameters, a 15% uncertainty about the nominal value is assumed. The set of controller parameters used in the simulation is given in Table IV. The vehicle is commanded to perform a simultaneous step change in both the x and z coordinates from an initial configuration $(x_0, \dot{x}_0) = (0,0)$, $(z_0, \dot{z}_0) = (0,0)$, $(\theta_0, \dot{\theta}_0) = (\pi/8, 0)$ to the desired set point $x_d = 10$ [m], $z_d = -5$ [m], with $\theta^\star$. Since $\lambda_r = \pi/4$, in this case the trim value for θ is $\theta = \pi/4$ as well. Since the reference frame is assumed positive downward, this maneuver corresponds to the vehicle raising its initial altitude while translating forward. Simulation results for the longitudinal and vertical motion are shown in Fig. 2 and Fig. 3, respectively. The vehicle position converges asymptotically to the set point in about 25 [s]. Notice the limit attained by the vertical velocity within $t \in [1.2, 7.5]$ [s] due to the saturated control law. Figure 4 shows that during the maneuver the internal pitch dynamics remain well-behaved, and asymptotic convergence to the equilibrium value is observed. The behavior of the physical control inputs, $\delta(t)$ and $\lambda(t)$, is shown in Fig.5. The unknown steady-state correction required to maintain the vehicle in hover is seen in the long term behavior of $\delta(t)$. In addition, $\lambda(t)$ quickly attains the trim value λ_*.

V. CONCLUSIONS

In this paper, we have presented the design of a robust nonlinear controller to globally stabilize the averaged longitudinal model of an under-actuated flapping-wing MAV to a constant desired configuration. In terms of the original, non-averaged, dynamics, this control objective corresponds to the stabilization of a periodic orbit at hovering. The methodology discussed in this paper constitute a radical improvement with respect to earlier designs [10], which did not adequately address the non-minimum phase characteristic of the dynamics, and successfully extends to the 3-DOF case the methodology outlined in [8] for a 1-DOF vehicle model.

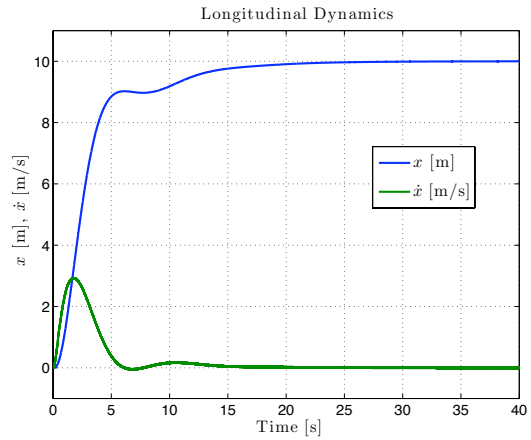

Fig. 2. Simulation results: Longitudinal motion $(x(t), \dot{x}(t))$.

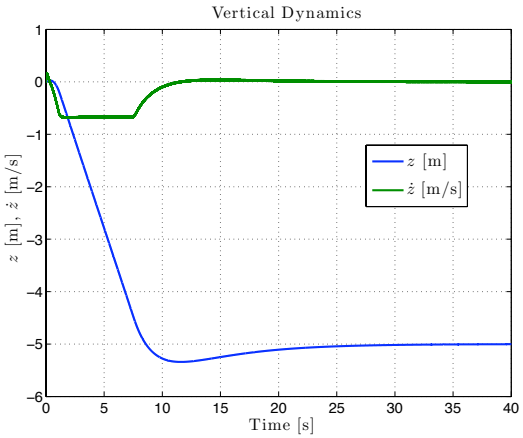

Fig. 3. Simulation results: Vertical motion $(z(t), \dot{z}(t))$.

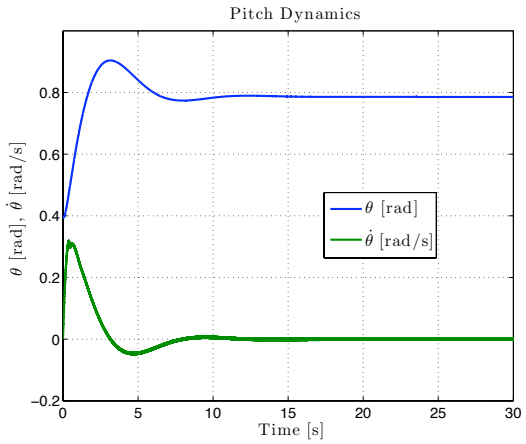

Fig. 4. Simulation results: Pitch dynamics $(\theta(t), \dot{\theta}(t))$

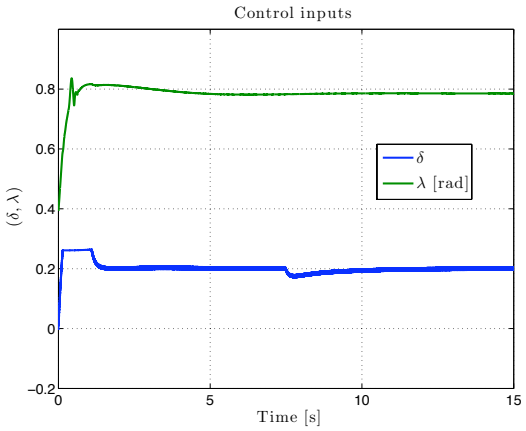

Fig. 5. Simulation results: Physical control inputs $(\delta(t), \lambda(t))$

ACKNOWLEDGMENTS

The author expresses his gratitude to Drs. Siva Banda, Dave Doman and Mike Bolender at AFRL/RBCA for their kind hospitality and assistance.

REFERENCES

[1] R. Madangopal and ZA Khan. Energetics-based design of small flapping-wing micro air vehicles. *IEEE/ASME Transactions on Mechatronics*, 11(4):433–438, 2006.

[2] J. Ratti and G. Vachtsevanos. A biologically-inspired micro aerial vehicle. *Journal of Intelligent & Robotic Systems*, 60(1):153–178, April 2010.

[3] S.P. Sane. The aerodynamics of insect flight. *Journal of Experimental Biology*, 206(23):4191–4208, 2003.

[4] X. Deng, L. Schenato, W.C. Wu, and S.S. Sastry. Flapping flight for biomimetic robotic insects: Part I-system modeling. *IEEE Transactions on Robotics*, 22(4):776, 2006.

[5] X. Deng, L. Schenato, and S.S. Sastry. Flapping flight for biomimetic robotic insects: Part II-flight control design. *IEEE Transactions on Robotics*, 22(4):789, 2006.

[6] D.B. Doman, M.W. Oppenheimer, and D.O. Sigthorsson. Wingbeat shape modulation for flapping-wing micro-air-vehicle control during hover. *Journal of Guidance, Control, and Dynamics*, 33(3):724–739, 2010.

[7] M.W. Oppenheimer, D.B. Doman, and D.O. Sigthorsson. Dynamics and control of a biomimetic vehicle using biased wingbeat forcing functions. *Journal of Guidance, Control, and Dynamics*, 34(1):204–217, January 2011.

[8] A. Serrani. Robust hovering control of a single-DOF flapping wing MAV. In *Proceedings of the American Control Conference*, Baltimore, MD, 2010.

[9] M.A. Bolender. Rigid multi-body equations-of-motion for flapping wing MAVs using Kane's equations. In *Proceedings of the AIAA Guidance, Navigation and Control Conference*, Chicago, IL, 2009.

[10] A. Serrani, B. E. Keller, M. A. Bolender, and D. B. Doman. Robust control of a 3-DOF flapping wing micro air vehicle. In *Proceedings of the AIAA Guidance, Navigation and Control Conference*, Toronto, ON, 2010.

[11] M. Bolender. Open-loop stability of flapping flight in hover. In *Proceedings of the AIAA Guidance, Navigation and Control Conference*, Toronto, ON, 2010.

[12] L. Marconi and A. Isidori. Robust global stabilization of a class of uncertain feedforward nonlinear systems. *Systems & Control Letters*, 41:281–290, 2000.

[13] A. Isidori, L. Marconi, and A. Serrani. *Robust Autonomous Guidance: An Internal Model-Based Approach*. Advances in Industrial Control. Springer Verlag, London, UK, 2003.

[14] W. Liu, Y. Chitour, and E.D. Sontag. On finite-gain stabilizability of linear systems subject to input saturation. *SIAM Journal on Control and Optimization*, 34(4):1190, 1996.

[15] A.R. Teel. A nonlinear small gain theorem for the analysis of control systems with saturations. *IEEE Transactions on Automatic Control*, 41(9):1256–1270, 1996.